

Synthesis and Characterization of Poly(HPMA)-APMA-DTPA-^{99m}Tc for Imaging-Guided Drug Delivery in Hepatocellular Carcinoma

Jianchao Yuan,¹ Chengping Miao,¹ Fangyu Peng,² Xianwu Zeng,³ Hongyun Guo,³
Xiaoqi Wang,³ Shiqi Liao,³ Xiaoli Xie¹

¹Key Laboratory of Eco-Environment-Related Polymer Materials of Ministry of Education, Key Laboratory of Polymer Materials of Gansu Province, College of Chemistry & Chemical Engineering, Northwest Normal University, Lanzhou 730070, China

²Department of Radiology and Advanced Imaging Research Center, University of Texas Southwestern Medical Center, 5323 Harry Hines Blvd, Dallas, Texas 75390-8542

³The PET Center, Department of Nuclear Medicine, Gansu Academy of Medical Sciences & Gansu Provincial Tumor Hospital, Lanzhou 730050, China

Correspondence to: J. Yuan (E-mail: jianchaoyuan@nwnu.edu.cn)

ABSTRACT: To develop a theranostic agent for diagnostic imaging and treatment of hepatocellular carcinoma (HCC), poly(HPMA)-APMA-DTPA-^{99m}Tc (HPMA: *N*-(2-hydroxypropyl methacrylamide); APMA: *N*-(3-aminopropyl)methacrylamide; DTPA: diethylenetriaminepentaacetic acid) and DTPA-^{99m}Tc were synthesized and characterized, and their HCC targeting was tested by *in vitro* cellular uptake and *in vivo* tumor imaging in this study. Radioactivity of HCC cells incubated with poly(HPMA)-APMA-DTPA-^{99m}Tc was significant higher (16.40%) than that of the cells incubated with DTPA-^{99m}Tc (2.98%). Scintigraphic images of HCC in mice obtained at 8 h after injection of poly(HPMA)-APMA-DTPA-^{99m}Tc showed increased radioactivity compared with that in mice injected with DTPA-^{99m}Tc. The results of postmortem tissue radioactivity assay demonstrated higher radioactivity of HCC tumor tissues (2.69 ± 0.15% ID/g) from the tumor-bearing mice injected with poly(HPMA)-APMA-DTPA-^{99m}Tc compared with that of HCC tumor tissues in the tumor-bearing mice injected with DTPA-^{99m}Tc (0.83 ± 0.03 %ID/g), (*P* < 0.001). These results first directly confirm the significant passive hepatocellular tumor targeting of HPMA copolymer. © 2012 Wiley Periodicals, Inc. *J. Appl. Polym. Sci.* 000: 000–000, 2012

KEYWORDS: hepatocellular carcinoma; passive targeting; HPMA copolymers; radiotracer; drug delivery

Received 21 February 2012; accepted 14 May 2012; published online

DOI: 10.1002/app.38065

INTRODUCTION

Hepatocellular carcinoma (HCC) is the fifth most frequently diagnosed cancer worldwide and the second most frequent cause of cancer death in men worldwide. In women, it is the seventh most commonly diagnosed cancer and the sixth leading cause of cancer death.¹ Evidence shows that 30–40% all cancers deaths can be prevented, and one-third can be cured through early diagnosis and treatment.² Early detection and classification of human tumors is one of the major goals in the fight to overcome cancer. Positron emission tomography (PET) molecular imaging allows repeated *in vivo* measurement of many critical molecular features of neoplasm, such as metabolism, proliferation, angiogenesis, hypoxia, and apoptosis, which can be used for monitoring therapeutic response. Particularly, as targeted therapies have become standard components of several cancer regimens, the ability to monitor the effect of these molecules

clinically through noninvasive imaging techniques has become of great interest. Therefore, continued validation is required for targeting radiotracers that go beyond FDG PET to measure the full extent of cancer cell physiology.³

N-(2-hydroxypropyl methacrylamide (HPMA) copolymers are biocompatible, nonimmunogenic, and nontoxic,⁴ and their body distribution is well characterized.⁵ HPMA copolymers accumulate selectively in tumor sites because of the enhanced permeation and retention (EPR) effect⁶, thus overcoming limitations of drug-related toxicities.⁷ The EPR phenomenon of passive diffusion through permeable neovasculature and localization in tumor interstitia is observed for macromolecular agents and lipids in many solid tumors. This passive phenomenon occurs because of tumor vasculature hyperpermeability (allowing polymer extravasation), and the lack of tumor tissue lymphatic drainage which subsequently promotes the retention of polymeric drugs.⁸

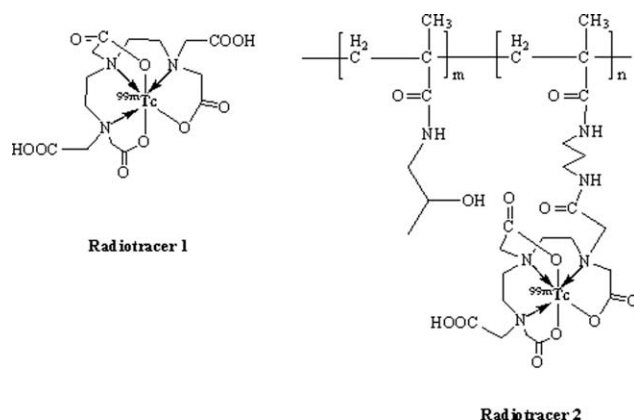


Figure 1. Chemical Structures of the radiotracers DTPA- ^{99m}Tc and Poly(HPMA)-DTPA- ^{99m}Tc .

Many previous reports have addressed the biocompatibility, the versatility, and the therapeutic potential of HPMA copolymers.^{9–20} Obviously, the passive targeting effect was very important for HPMA copolymer drugs and radiotracers. However, no report has directly compared the impact of the small molecular radiotracer [diethylenetriaminepentaacetic acid (DTPA- ^{99m}Tc)] modified with poly(HPMA) [e.g., poly(HPMA)-*N*-(3-aminopropyl)methacrylamide (APMA)-DTPA- ^{99m}Tc : only passive tumor targeting] on the biodistribution of hepatoma tumor-bearing mice. We, therefore, decided to investigate how the incorporation of poly(HPMA)-APMA reflects on the biodistribution and the tumor-targeting potential of DTPA- ^{99m}Tc .

We first coupled poly[APMA] with the macrocyclic, 1,4,7,10-tetraazacyclododecane-1,4,7,10-tetraacetic acid (DOTA) and labeled the poly[APMA]-DOTA conjugate with ^{64}Cu for radionuclide therapy and tumor targeting.²¹ Prolonged retention of poly[APMA]-DOTA- ^{64}Cu conjugates within the tumor tissues was demonstrated by micropositron emission tomography. In this study, we conjugated DTPA with the biocompatible, non-immunogenic, and nontoxic HPMA polymer and labeled the poly(HPMA)-APMA-DTPA conjugate with ^{99m}Tc for tumor targeting *in vitro* and *in vivo* on HCC (Figure 1). Cellular uptakes of the conjugates polyHPMA-DTPA- ^{99m}Tc and DTPA- ^{99m}Tc were examined by MTT assay on mouse hepatoma H22 cell line. The targeting efficacy, biodistribution, and retention of the conjugates poly(HPMA)-APMA-DTPA- ^{99m}Tc and DTPA- ^{99m}Tc were investigated on mice bearing hepatoma cancer.

EXPERIMENTAL

Materials

HPMA and APMA were purchased from Polyscience (Warrington, PA). Thionyl chloride, 2,2'-azobisisobutyronitrile (AIBN), and DTPA were purchased from Sigma-Aldrich. Dimethyl sulfoxide and acetone were predried with 4 Å molecular sieves and distilled from CaH_2 under dry nitrogen.

Radioactive $\text{Na}^{99m}\text{TcO}_4$ was obtained from the $^{99}\text{Mo}/^{99m}\text{Tc}$ generator (Beijing Atom HighTech China). The mouse hepatoma H22 cell line was obtained from Gansu Academy of Medical Sciences and Gansu Provincial Tumor Hospital (Lanzhou, China). Animal experiments were performed in KunMing mice

(male; average weight, ~ 20 g) obtained from the Animal Center of Lanzhou University (Lanzhou, China). All biodistribution studies were performed under a protocol approved by the Lanzhou Administration Office of Laboratory Animal.

NMR spectra were recorded on a Varian Mercury plus-400 instrument, using TMS as internal standard. The molecular weights and molecular weight distributions of the polymers were determined by gel permeation chromatography/size exclusion chromatography via a Waters Alliance GPCV 2000 chromatograph equipped with refractive index, differential viscometer, and light scattering (90, RALLS) detectors, using 0.2 M NaNO_3 , 0.01 M NaH_2PO_4 (pH 7) as the eluent, at a flow rate of 1.0 mL/min and 30°C.

Synthesis of APMA-DTPA Monomer (1)

The operations were carried out under N_2 atmosphere using standard Schlenk techniques. Thionyl chloride (0.12 g, 1.02 mmol) was slowly added to a stirred solution of DTPA (0.44 g, 1.12 mmol) in dimethyl sulfoxide (DMSO, 2 mL) at room temperature. Then, the mixture was stirred for 5 h at 60°C, then cooled and precipitated with CH_2Cl_2 (20 mL). The precipitate was separated by filtration and dried under vacuum at room temperature to give the activated DTPA. The activated DTPA was dissolved in DMSO (1 mL), and APMA (0.14 g, 1.0 mmol) was added. The mixture was stirred for 48 h at room temperature. The solution was added slowly to cooled (ice-salt bath) CH_2Cl_2 (20 mL) with stirring. The precipitate was filtered off, washed with CH_2Cl_2 thoroughly, and dried at room temperature under vacuum. The precipitate was recrystallized from methanol, washed with cold methanol, and dried under vacuum to give monomer 1. Yield: 0.33 g, 64%. ^1H NMR (400 MHz, D_2O , δ , ppm): 5.85 (s, 1H, Proton1), 5.61 (s, 1H, Proton1), 3.80 (s, 8H, Proton2), 3.53 (m, 4H, Proton3), 3.40 (t, 4H, Proton4), 3.22 (t, 4H, Proton5), 3.16 (m, 2H, Proton6), 2.07 (m, 5H, Proton7 and Proton8). ^{13}C NMR (400 MHz, D_2O , δ , ppm): 179.1 (Carbon1), 175.5 (Carbon2), 174.4 (Carbon3), 141.1 (Carbon4), 125.7 (Carbon5), 59.7 (Carbon6), 58.4 (Carbon7), 54.2 (Carbon8), 52.2 (Carbon9), 39.2 (Carbon10), 38.5 (Carbon11), 28.98 (Carbon12), 19.9 (Carbon13). Figures 3 and 4 show the serial number of protons and carbons.

Synthesis of Poly(HPMA)-APMA-DTPA Conjugate (2)

Acetone (3 mL), DMSO (3 mL), HPMA (143 mg, 1.00 mmol), monomer 1 (60 mg, 0.12 mmol), and AIBN (10 mg, 0.006 mmol) were introduced into a 10 mL of ampule and stirred at room temperature to give a homogeneous solution. The reaction mixture was sealed under vacuum after deoxygenation by three cycles of nitrogen/vacuum in a dry ice bath. The polymerization was carried out at 60°C for 24 h. Then, the reaction mixture was cooled to room temperature and filtered. The polymer conjugates (<20000 or >40000) were removed by centrifuge filtration using a Vivaspine 2 spin column (MWCO 20 or 40 kDa, Vivascience, Hannover, Germany); the polymer conjugates (20000–40000) lyophilized to dryness giving poly(HPMA)-DTPA conjugate as pale yellow powder (98 mg, 48%). ^1H NMR (400 MHz, D_2O , δ , ppm): 3.83 (Proton1), 3.68 (Proton2), 3.47 (Proton3), 3.29 (Proton4), 2.86–3.00 (Proton5,6,7,8), 1.54–1.64 (Proton9,10), 0.75–0.96 (Proton11,12,13). ^{13}C NMR (400 MHz,

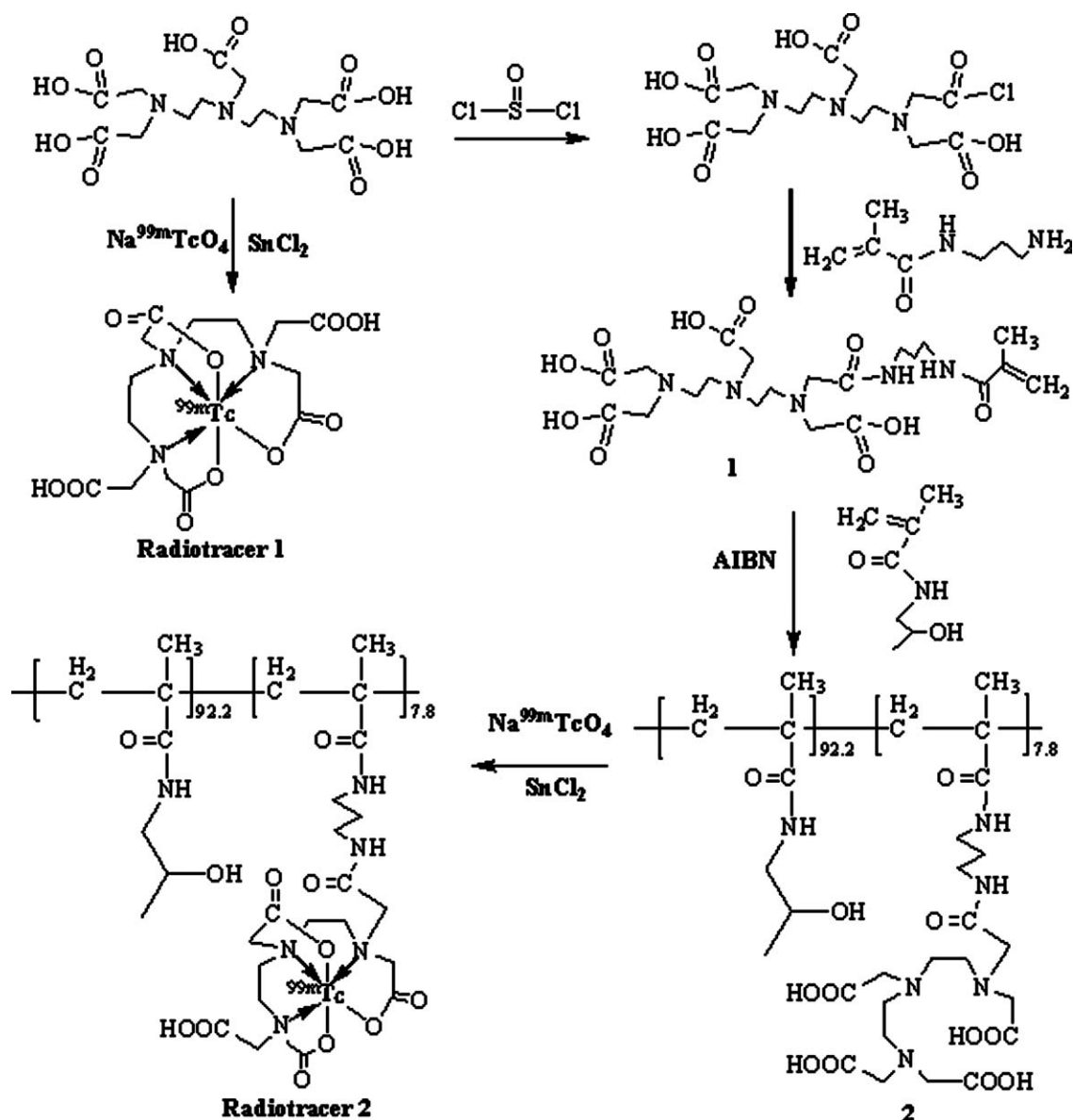


Figure 2. Synthetic scheme of the DTPA- $^{99\text{m}}\text{Tc}$ and poly(HPMA)-DTPA- $^{99\text{m}}\text{Tc}$ conjugates.

DMSO- d_6 , δ , ppm): 177.52 (Carbon1), 177.18 (Carbon2), 176.43 (Carbon3), 173.09 (Carbon4), 65.02 (Carbon5), 55.41 (Carbon6), 54.74 (Carbon7), 54.41 (Carbon8), 52.40 (Carbon9), 48.98 (Carbon10), 47.56 (Carbon11), 45.88 (Carbon12), ~ 39 (Carbon13, overlap with DMSO), ~ 38 (Carbon14, overlap with DMSO), 25.41 (Carbon15), 21.65 (Carbon16), 19.64 (Carbon17), 16.21 (Carbon18). The serial number of protons and carbons shows in Figure 5 and Figure 6. M_n : 2.2×10^4 , M_w/M_n : 1.38.

Radiolabeling of Poly(HPMA)-APMA-DTPA Conjugates with $^{99\text{m}}\text{Tc}$ Radionuclide

Poly(HPMA)-APMA-DTPA conjugates were radiolabeled with $^{99\text{m}}\text{Tc}$ radionuclide by adding $\text{Na}^{99\text{m}}\text{TcO}_4$ into a solution of DTPA and poly(HPMA)-APMA-DTPA conjugates in 2 mL of 0.1 M sodium acetate buffer (pH 5.5) and incubating at room temperature for 30 min in the presence of SnCl_2 . The labeled

poly(HPMA)-APMA-DTPA- $^{99\text{m}}\text{Tc}$ conjugates were purified by centrifuge filtration using Vivaspin 2 (MWCO 3 kDa, Vivascience, Hannover, Germany) to separate the conjugates from free $^{99\text{m}}\text{Tc}$ using distilled water as the solvent. Specific activity ($\mu\text{Ci}/\text{mg}$) of the poly(HPMA)-APMA-DTPA- $^{99\text{m}}\text{Tc}$ conjugates were determined by measuring the radioactivity of the conjugates purified with the Vivaspin column. Radiolabeling efficiency was determined by dividing the radioactivity of the purified radiolabeled conjugates by the total radioactivity of the conjugates and the filtrates containing nonconjugated free $^{99\text{m}}\text{Tc}$ radionuclide and then multiplying by 100.

The radiochemical purity of the $^{99\text{m}}\text{Tc}$ -labeled conjugates was also determined using instant thin-layer chromatography. Ethyl acetate, water, and ethanol (5 : 5 : 2, v/v/v) were mixed with stirring. The ester phase and water phase were separated after standing for 5–10 min. The radiochemical purity of the labeled

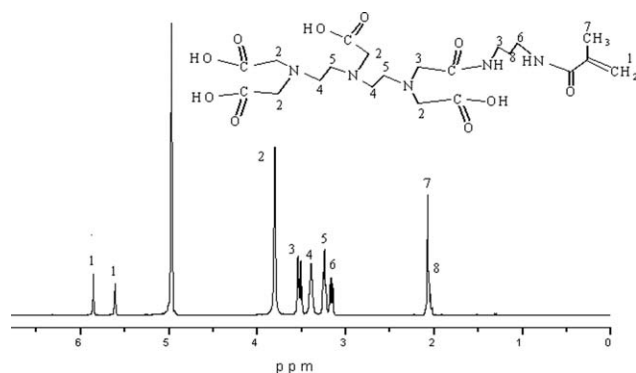


Figure 3. ^1H NMR (400 MHz, D_2O) spectrum of monomer APMA-DTPA.

DTPA- $^{99\text{m}}\text{Tc}$ and poly(HPMA)-DTPA- $^{99\text{m}}\text{Tc}$ conjugates was determined using instant thin-layer chromatography (No. 1 Xinhua filter paper, Hangzhou Xinhua Group China) with ester phase and water phase as the developing solvent, respectively (ester phase: $^{99\text{m}}\text{Tc}$ -labeled DTPA conjugates $R_f \sim 0$, $\text{Na}^{99\text{m}}\text{TcO}_4$ $R_f \sim 0.5$; water phase: $^{99\text{m}}\text{Tc}$ -labeled DTPA conjugates $R_f \sim 0.9$, $\text{Na}^{99\text{m}}\text{TcO}_4$ $R_f \sim 0$).

Finally, the radiolabeled conjugates dissolved in normal saline were sterilized by filtration with a 0.22 mm millipore filter before use in animal studies. Radiolabeling of DTPA with Tc-99 m was conducted in a same fashion and used as control.

Cellular Uptake Assay of Poly(HPMA)-APMA-DTPA- $^{99\text{m}}\text{Tc}$ *In Vitro*

In the time-dependent uptake study, DTPA- $^{99\text{m}}\text{Tc}$ and poly(-HPMA)-APMA-DTPA- $^{99\text{m}}\text{Tc}$ prepared as described were diluted in 0.5 mL of RPMI 1640 medium (RPMI: Roswell Park Memorial Institute), and 0.15 μCi ($\sim 0.75 \mu\text{g}$) was added to monolayers of H22 cells grown in 35 mm tissue culture dishes. The cells were incubated at 37°C for different lengths of time, washed with $3 \times 1 \text{ mL}$ of cold phosphate buffered saline (PBS: , 136.9 mM NaCl, 2.68 mM KCl, 8.1 mM Na_2HPO_4 , 1.47 mM KH_2PO_4 , pH 7.4) and then suspended in 1 mL of PBS by scraping. The amount of cell-associated radioactivity was determined using an automatic γ -counter. Cellular protein content was measured by the bicinchoninic acid (BCA) protein assay.

Nuclear Imaging of Biodistribution of Poly(HPMA)-APMA-DTPA- $^{99\text{m}}\text{Tc}$ Conjugates (in Mice Bearing Extrahepatic Hepatoma Grafts)

Animal studies were performed according to a protocol approved by the Lanzhou Administration Office of Laboratory Animal. H22 mouse hepatoma cancer cells (Hepatoma (H22) cells were provided by Gansu Academy of Medical Sciences and Gansu Provincial Tumor Hospital, Lanzhou, China) were cultured in RPMI 1640 medium supplemented with 10% fetal bovine serum, 100 U/mL penicillin, and 100 mg/mL streptomycin. To establish extrahepatic mouse hepatoma grafts, H22 cells (5×10^6 /injection site) were injected to a right flank of a mouse (male, 4–5 weeks old) purchased from the Animal Center of Lanzhou University (Lanzhou, China). When the hepatoma xenografts reached about $0.8 \times 0.8 \text{ cm}^2$ in size, the tumor-bearing

mice were subjected to nuclear imaging after intravenous injection of the radiolabeled conjugates.

The tumor-bearing mice were anesthetized with a mixture of ketamine (100 mg/kg) and xylazine (7 mg/kg), and the poly (HPMA)-APMA-DTPA- $^{99\text{m}}\text{Tc}$ conjugates (200–500 mCi in 0.1 mL normal saline) were injected via the tail vein. The tumor-bearing mice in control group were injected with same dose of DTPA- $^{99\text{m}}\text{Tc}$. Static data acquisition was performed at 8 h postinjection using a dual head gamma camera with a low energy all purpose collimator (SPECT-CT, General Electric Co.). At the time of euthanasia, blood samples were collected by cardiac puncture. During necropsy, whole organ tissue samples were obtained from the heart, lung, liver, spleen, kidney, muscle, and tumor. The tissue samples were washed with water, counted (Zhongjia-1200 γ -counter, Zhongjia Guandian Co. China), and weighed and the percentage injected dose per gram tissue (% ID/g) was calculated. All biodistribution studies were performed with three mice per group.

Statistical Analysis

Values are presented as mean \pm SD. An unpaired two-tailed t test was used to determine statistical significance using GraphPad InStat software (GraphPad Software). A P value of less than 0.05 was considered statistically significant.

RESULTS AND DISCUSSION

Synthesis and Characterization of DTPA- $^{99\text{m}}\text{Tc}$ and Poly(HPMA)-APMA-DTPA- $^{99\text{m}}\text{Tc}$ Conjugates

The synthetic pathway for the DTPA- $^{99\text{m}}\text{Tc}$ and poly(HPMA)-APMA-DTPA- $^{99\text{m}}\text{Tc}$ conjugates is shown in Figure 2. The radio-tracer monomer was synthesized in two steps: (1) DTPA (chelator) reacted with thionyl chloride, because of its multivalent nature, an excess of DTPA was used to ensure that only one carboxylic acid group is activated and that no undesired cross-linking takes place in the reaction with APMA; (2) the resulting DTPA-Cl was reacted with APMA to form monomer APMA-DTPA via a stable amide bond. The ^1H NMR and ^{13}C NMR spectra are shown in Figures 3 and 4.

The polymer conjugates, poly(HPMA)-APMA-DTPA, were synthesized by a conventional free radical precipitation poly-

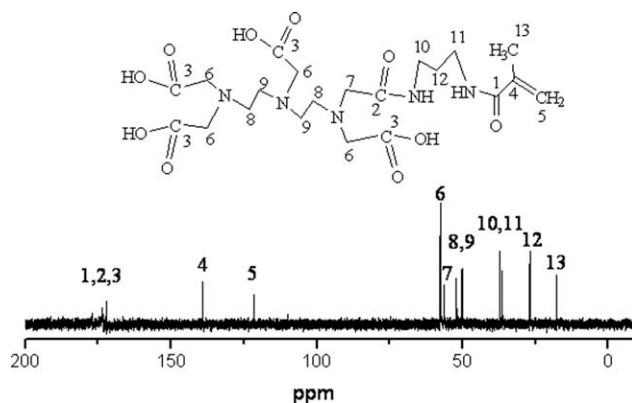


Figure 4. ^{13}C NMR (400 MHz, D_2O) spectrum of monomer APMA-DTPA.

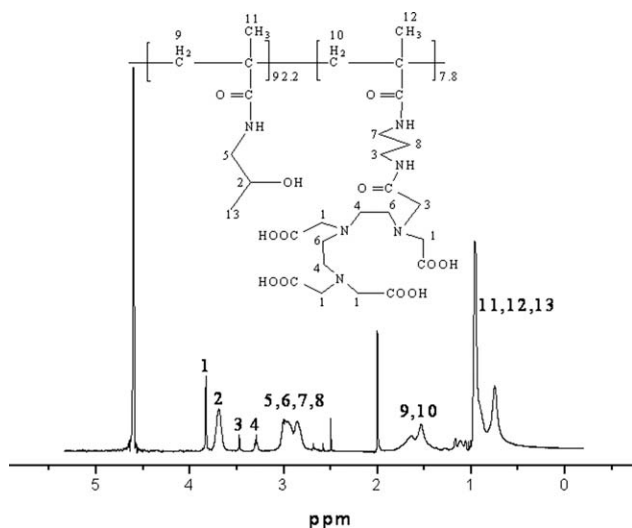


Figure 5. ^1H NMR (400 MHz, D_2O) spectrum of poly(HPMA)-APMA-DTPA.

merization, and the polymerization conditions, such as initiator concentration, were optimized to obtain polymers with the desired molecular weight.⁴ Simple centrifuge filtration was sufficient to purify the poly(HPMA)-APMA-DTPA conjugates from unreacted monomers and other low-molecular weight byproducts. Poly[HPMA] is not a biodegradable polymer, so the target

molecular weight (20,000–40,000 g/mol) was selected to ensure ultimate renal elimination (The polymer conjugates (<20000 or >40000) were removed by centrifuge filtration using a Vivaspin 2 spin column (MWCO 20 or 40 kDa, Vivascience, Hannover, Germany)).²² The ^1H NMR and ^{13}C NMR spectra are shown in Figures 5 and 6.

The purified poly(HPMA)-APMA-DTPA conjugates were characterized by ^1H -NMR to determine the content of DTPA groups in the conjugates (Figure 5). We have used the integral intensities of the $-\text{CH}_2-\text{COOH}$ protons of DTPA (3.83 ppm) and the integral intensity of the $\text{CH}_3-\text{CH}(\text{OH})-\text{CH}_2-\text{NH}-$ protons of the HPMA (3.68 ppm) to calculate the content of DTPA in the Poly(HPMA)-DTPA conjugates ($\text{DTPA mol\%} = I_{3.83}/(I_{3.68} + I_{3.83}/8) \times 100\%$. $I_{3.83}$: the integral intensities of the $-\text{CH}_2-\text{COOH}$ protons of DTPA; $I_{3.68}$: the integral intensity of the $\text{CH}_3-\text{CH}(\text{OH})-\text{CH}_2-\text{NH}-$ protons of the HPMA). The data show that, on average, the poly[HPMA]-APMA-DTPA conjugates contained 7.8 mol% of the monomer units modified with DTPA. Assuming the molecular weight of poly[HPMA]-APMA-DTPA to be 22,000 daltons, it translates into 10 DTPA groups per average polymer chain.

Finally, the DTPA and poly(HPMA)-APMA-DTPA conjugates were radiolabeled with $^{99\text{m}}\text{Tc}$ radionuclide by incubation of the conjugates with $\text{Na}^{99\text{m}}\text{TcO}_4$ in 2 mL of acetate buffer (pH 5.5) at room temperature for 30 min in the presence of SnCl_2 . Specific activities of DTPA- $^{99\text{m}}\text{Tc}$ and poly(HPMA)-APMA-DTPA- $^{99\text{m}}\text{Tc}$ conjugates were estimated at 200–300 $\mu\text{Ci/}$

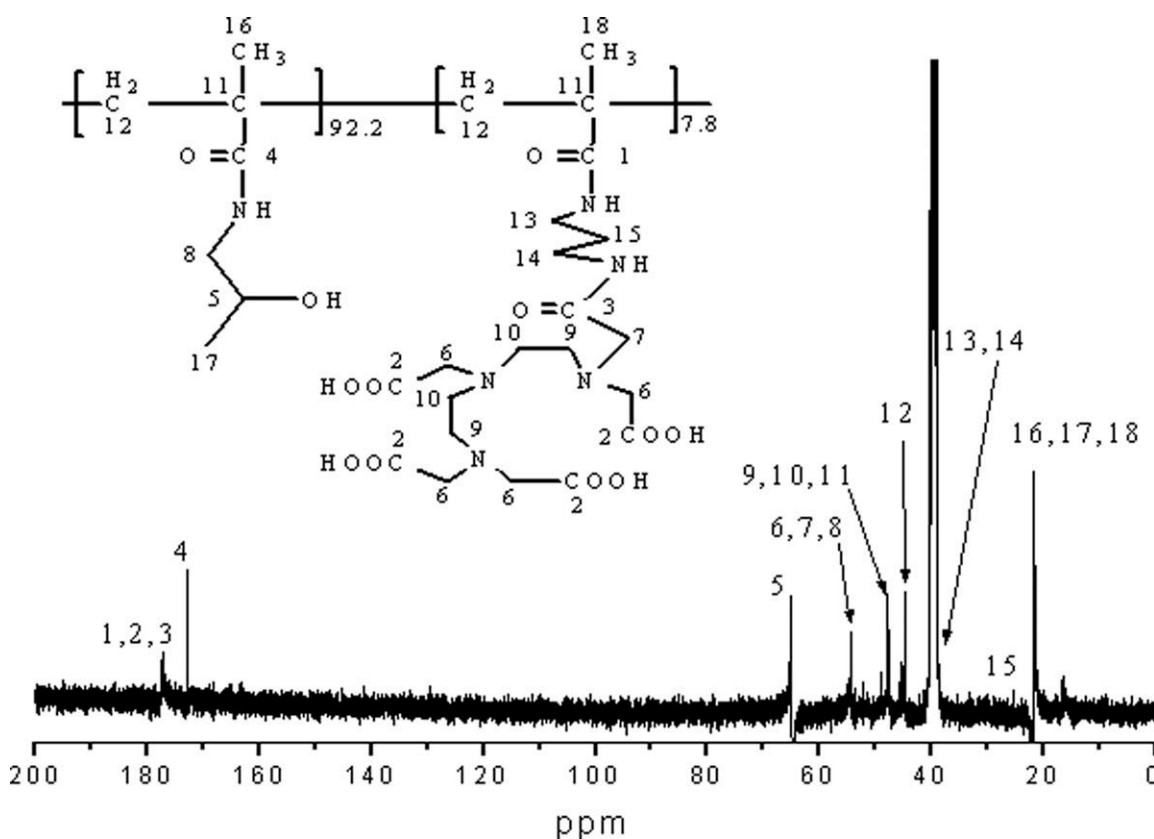


Figure 6. ^{13}C NMR (400 MHz, DMSO-d_6) spectrum of poly(HPMA)-APMA-DTPA.

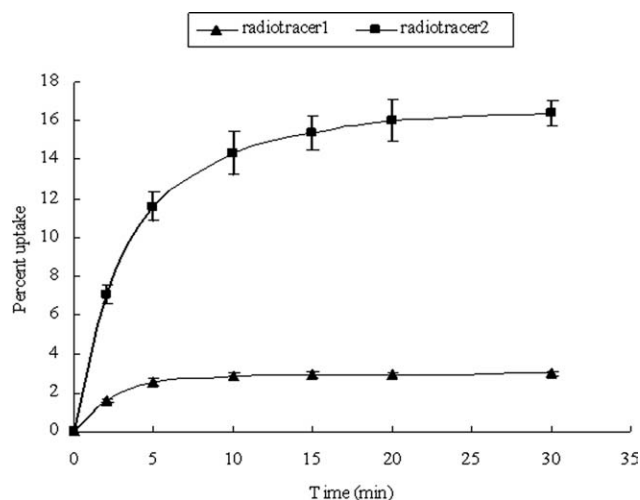


Figure 7. Kinetics of association of poly(HPMA)-APMA-DTPA- ^{99m}Tc and DTPA- ^{99m}Tc with cultured H22 cells at 37°C. H22 cells were incubated for the indicated times with 0.15 μCi poly(HPMA)-APMA-DTPA- ^{99m}Tc (■) and DTPA- ^{99m}Tc (▲) at 37°C. After the cells were washed with 3×1 mL of cold PBS, the cells were suspended in 1 mL of PBS by scraping. The amount of cell-associated radioactivity was determined using a γ -counter, and cellular protein content was determined by BCA assay. Error bars represent standard deviations of three parallel experiments.

mg, ^{99m}Tc radiolabeling of the DTPA and copolymer conjugates achieved efficiencies of $>92\%$. After purification, the radiochemical purities of DTPA- ^{99m}Tc and poly(HPMA)-APMA-DTPA- ^{99m}Tc conjugates were 98.9% and 97.9%, respectively,

which were determined using instant thin-layer chromatography.

Increased Radioactivity of HCC Cells Incubated with Poly(HPMA)-APMA-DTPA- ^{99m}Tc

HCC cell H22 was used to investigate the *in vitro* passive binding of radiotracer 2 poly(HPMA)-APMA-DTPA- ^{99m}Tc , using DTPA- ^{99m}Tc radiotracer 1 as a control. The time dependence of internalization of the radiotracer 2 in H22 cells was evaluated. The H22 cells were incubated with 0.15 μCi of DTPA- ^{99m}Tc radiotracer 1 and poly(HPMA)-APMA-DTPA- ^{99m}Tc radiotracer 2 for 30 min and their relative activity was measured (Figure 7). Interestingly, the maximal uptake of poly(HPMA)-APMA-DTPA- ^{99m}Tc (passive binding) reached 16.40% of the total conjugate added. Perhaps, the high uptake is due to the lysosomotropic nature of HPMA copolymers.^{2,3}

As controls, DTPA- ^{99m}Tc lacking of passive targeted HPMA polymeric carrier did not show any significant cell association (2.98%, Figure 7). These results clearly demonstrated that the passive binding facilitate the delivery of ^{99m}Tc loaded poly(HPMA)-APMA-DTPA conjugates into H22 cells.

Visualization of Hepatoma on Scintigraphic Images of Tumor-bearing Mice Injected with Poly(HPMA)-APMA-DTPA- ^{99m}Tc

Scintigraphic images of mice bearing hepatoma tumor xenografts 8 h after injection are shown in Figure 8. The poly(HPMA)-APMA-DTPA- ^{99m}Tc radiotracer conjugates showed significantly higher tumor accumulation relative to DTPA- ^{99m}Tc radiotracer.

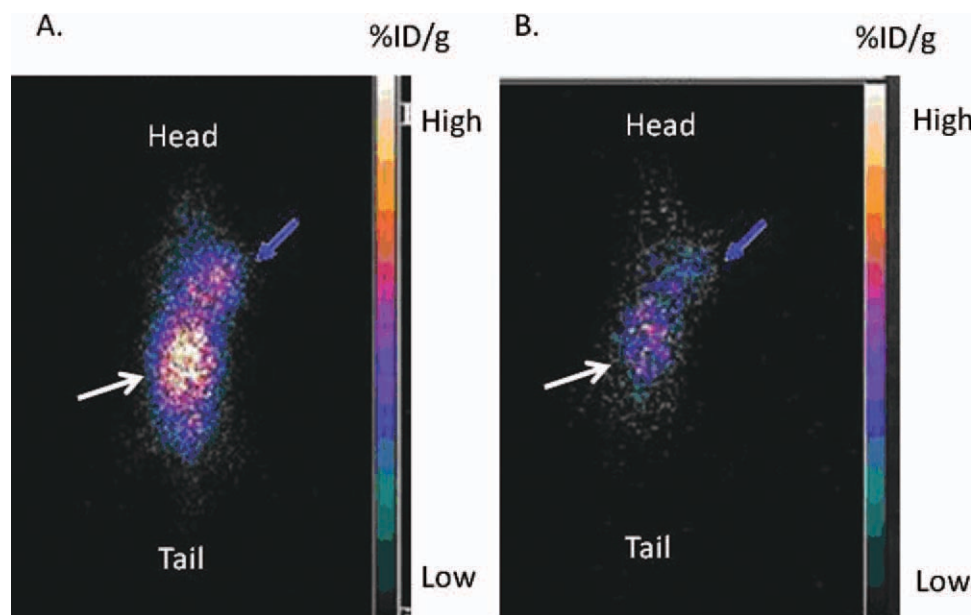


Figure 8. Scintigraphic images of tumor-bearing mice injected with poly(HPMA)-APMA-DTPA- ^{99m}Tc or DTPA- ^{99m}Tc . A: Scintigraphic images of tumor-bearing mice obtained at 8 h post injection of poly(HPMA)-APMA-DTPA- ^{99m}Tc ; B: Scintigraphic images of tumor-bearing mice obtained at 8 h post injection of DTPA- ^{99m}Tc . The poly(HPMA)-APMA-DTPA- ^{99m}Tc conjugates showed significantly higher tumor localization compared with that in the control tumor-bearing mice injected with DTPA- ^{99m}Tc . Blue arrows indicate the conjugates in the tumor tissue; white arrows indicate the conjugates in liver, spleen, and kidney tissues. [Color figure can be viewed in the online issue, which is available at wileyonlinelibrary.com.]

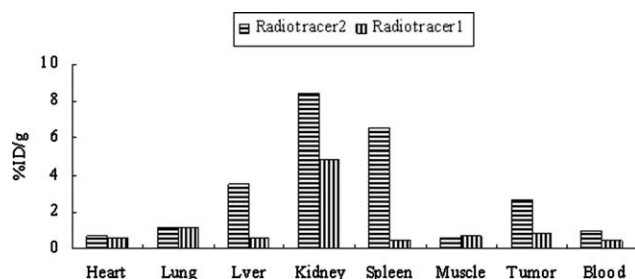


Figure 9. Residual radioactivity in %ID/g of organ tissue 24 h after intravenous injection of poly(HPMA)-APMA-DTPA-^{99m}Tc (Radiotracer 2) and DTPA-^{99m}Tc (Radiotracer 1) in H22 hepatoma tumor xenograft-bearing mice. Organ data are expressed as mean \pm SD.

The 24-h necropsy radioactivity was expressed as %ID/g. In the H22 xenograft model (Figure 9), poly(HPMA)-APMA-DTPA-^{99m}Tc ($2.69 \pm 0.15\%$ ID/g) showed significantly higher tumor accumulation ($P < 0.001$) than DTPA-^{99m}Tc ($0.83 \pm 0.03\%$ ID/g), indicating the passive targeting of poly(HPMA)-APMA-DTPA-^{99m}Tc. The blood activity of Poly(HPMA)-APMA-DTPA-^{99m}Tc ($0.973 \pm 0.017\%$ ID/g) was higher ($P < 0.001$) than DTPA-^{99m}Tc ($0.403 \pm 0.077\%$ ID/g), suggesting longer circulation times for the polymeric conjugates. This means that poly(HPMA)-APMA-DTPA-^{99m}Tc have significant passive targeting ability.

Biodistribution of Poly(HPMA)-APMA-DTPA-^{99m}Tc in Tumor-Bearing Mice by Postmortem Tissue Radioactivity Assay

To evaluate the targeting potential of poly(HPMA)-APMA-DTPA-^{99m}Tc, its ability to localize to hepatoma tumor was investigated. By dividing the tumor concentration of poly(HPMA)-APMA-DTPA-^{99m}Tc by its concentrations in healthy organs and tissues, tumor-to-organ ratios were calculated and they were used to allow for a more direct and cross-sectional comparison of the tumor-targeting ability of poly(HPMA)-APMA-DTPA-^{99m}Tc (Table I). A tumor-to-organ ratio >1 indicates that accumulation in tumor tissue was more effective, and a ratio <1 indicates an enhanced localization to healthy tissue. When interpreting all ratios macroscopically, it can be seen that for poly(HPMA)-APMA-DTPA-^{99m}Tc, a proper tumor-targeting ability was found. The tumor-to-organ ratios were found to be >1 for blood, lung, heart, and muscle (Tables I). Only for kidney, spleen, and liver ratios were <1 . For spleen, ratio was <1 , confirming the role of the spleen (and splenic macrophages) in clearing long-circulating drug delivery systems.²⁴ For kidney, ratio was also <1 , indicating that the copolymers were cleared from the circulation more rapidly. Relative levels in liver were generally comparable to levels in tumor. As poly(HPMA)-DTPA are nondegradable, most of them will be eliminated in liver. This is why the activity in liver was larger than other tissues when poly(HPMA)-APMA-DTPA-^{99m}Tc conjugates were injected into mouse (Figure 8).

In this study, the HPMA copolymer was used to achieve passive delivery because of their neutral charge; high water solubility; and ease of synthesis, modification, and incorporation of drugs. The lysosomotropic nature of HPMA copolymers²³ was found

to be able to guide the DTPA-^{99m}Tc to reach its target, both *in vitro* and *in vivo* (Figures 7 and 8).

The delivery of macromolecules to their target site is currently the limiting factor for many large compounds. Macromolecules have generally been considered to be impermeable to cell membranes and enter cells via endocytosis.^{25,26} The endocytosed macromolecules remain in membrane-bound vesicles,²⁷ unless some type of permeation enhancer (eg, fusogenic peptides²⁸ or cell-penetrating peptides²⁹) is used. Our study of H22 cell uptake of poly(HPMA)-APMA-DTPA-^{99m}Tc revealed that the complex is bound and enters cells via endocytosis. The uptake kinetics is fast, reaching 50% maximal cell association (16.40%) in ~ 5 min (Figure 7), suggesting that Poly(HPMA)-APMA-DTPA-^{99m}Tc might be useful as a radiopharmaceutical for tumor imaging.

Many studies have led to a general understanding of the fate of HPMA copolymers, especially *in vivo*.^{27,30,31} HPMA copolymers with molecular weights below the renal threshold³² are rapidly cleared from the blood.³³ Higher molecular weight polymers have a longer blood residence time, and no unexplainable amounts of copolymer accumulate in organs.³² An increase in the molecular weight of macromolecules also leads to passive targeting in tumors because of the EPR effect.³¹

Though a pronounced localization to liver and to kidney may intuitively seem disadvantageous, this could just be used to argue for a broader implementation of HPMA copolymers in the treatment of advanced solid malignancies. Because the carrier constructs tend to concentrate in liver tissue relatively effective, HPMA copolymer-based radiotracers or anticancer agents may well provide more effective means for monitoring and treating both primary and secondary liver lesions. The same is true for kidney cancer, which in spite of extensive research efforts remains to be one of the most lethal malignancies.³⁴ HPMA copolymers were shown to possess an intrinsic ability to accumulate in kidney. It can, therefore, be expected that they will be able to increase the levels of radiotracers or therapeutic agents in the kidney substantially.³⁵

CONCLUSIONS

A radiotracer passive delivery system was developed based on poly(HPMA)-APMA-DTPA conjugate. The system consists of poly(HPMA) carrier, APMA-DTPA chelator, and radionuclide ^{99m}Tc. The radiotracer passive delivery system poly(HPMA)-

Table I. Tumor/Organ Ratios of Poly(HPMA)-DTPA-^{99m}Tc 24 h Postintravenous Injection

	Poly(HPMA)-DTPA- ^{99m} Tc
Heart	4.089685309
Lung	2.502601631
Liver	0.813364744
Kidney	0.340744346
Spleen	0.440513517
Muscle	4.699406412
Blood	2.950861335

APMA-DTPA-^{99m}Tc conjugate could be taken up by HCC cell H22 *in vitro* and HCC cells *in vivo*, respectively. Thus, the poly (HPMA)-APMA-DTPA-^{99m}Tc conjugate passive radiotracer delivery system was proven effectively both *in vitro* and *in vivo*.

ACKNOWLEDGMENTS

The authors thank the National Natural Science Foundation of China (20964003) for funding. They also thank Key Laboratory of Eco-Environment-Related Polymer Materials of Ministry of Education, Key Laboratory of Polymer Materials of Gansu Province (Northwest Normal University), for financial support.

REFERENCES

- Jemal, A.; Bray, F.; Center, M. M.; Ferlay, J.; Ward, E.; Forman, D. *CA Cancer. J. Clin.* **2011**, *61*, 69.
- WHO: The World Health Organization's Fight Against Cancer **2007**.
- Michalski, M. H.; Chen, X. *Eur. J. Nucl. Med. Mol. Imaging* **2011**, *38*, 358.
- Bilej, M.; Vetvicka, V.; Ulbrich, K.; Strohalm, J.; Kopecek, J.; Duncan, R. *Biomaterials* **1989**, *10*, 335.
- Seymour, L. W.; Ulbrich, K.; Strohalm, J.; Kopecek, J.; Duncan, R. *Biochem. Pharmacol.* **1990**, *39*, 1125.
- Maeda, H.; Wu, J.; Sawa, T.; Matsumura, Y.; Hori, K. *J. Controlled Release* **2000**, *65*, 271.
- Duncan, R.; Coatsworth, J. K.; Burtles, S. *Hum. Exp. Toxicol.* **1998**, *17*, 93.
- Matsumura, Y.; Maeda, H. *Cancer. Res.* **1986**, *46*, 6387.
- Duncan, R.; Vicent, M. J. *Adv. Drug Deliv. Rev.* **2010**, *62*, 272.
- Ulbrich, K.; Subr, V. *Adv. Drug Deliv. Rev.* **2010**, *62*, 150.
- Etrych, T.; Kovář, L.; Strohalm, J.; Chytil, P.; Říhová, B.; Ulbrich, K. *J. Controlled Release* **2011**, *154*, 241.
- Etrych, T.; Strohalm, J.; Chytil, P.; Černoch, P.; Starovoytova, L.; Pechar, M.; Ulbrich, K. *Eur. J. Pharm. Sci.* **2011**, *42*, 527.
- Pike, D. B.; Ghandehari, H. *Adv. Drug Deliv. Rev.* **2010**, *2*, 167.
- Ray, A.; Larson, N.; Pike, D. B.; Grüner, M.; Naik, S.; Bauer, H.; Malugin, A.; Greish, K.; Ghandehari, H. *Mol. Pharm.* **2011**, *4*, 1090.
- Satchi-Fainaro, R.; Puder, M.; Davies, J.; Tran, H.; Sampson, D.; Greene, A. K.; Corfas, G. *J. Nat. Med.* **2004**, *10*, 255.
- Ulbrich, K.; Subr, V. *Adv. Drug Deliv. Rev.* **2010**, *2*, 150.
- Kopeček, J.; Kopečková, P. *Adv. Drug Deliv. Rev.* **2010**, *2*, 122.
- Říhová, B.; Kovář, M. *Adv. Drug Deliv. Rev.* **2010**, *2*, 184.
- Kostkova, H.; Etrych, T.; Rhova, B.; Ulbrich, K. *J. Bioact Compat Polym.* **2011**, *26*, 270.
- Greish, K.; Ray, A.; Bauer, H.; Larson, N.; Malugin, A.; Pike, D.; Haider, M.; Ghandehari, H. *J. Controlled Release* **2011**, *3*, 263.
- Yuan, J.; You, Y.; Xin Lu, X.; Muzik, O.; Oupicky, D.; Peng, F. *Mol. Imaging* **2007**, *6*, 10.
- Seymour, L. W.; Miyamoto, Y.; Maeda, H.; Brereton, M.; Strohalm, J.; Ulbrich, K.; Duncan, R. *Eur. J. Cancer.* **1995**, *31*, 766.
- Omelyanenko, V.; Kopečková, P.; Gentry, C.; Kopecek, J. *J. Controlled Release* **1998**, *53*, 25.
- Lammersa, T.; Kühnlein, R.; Kissel, M.; Subr, V.; Etrych, T.; Pola, R.; Pechar, M.; Ulbrich, K.; Storm, G.; Huber, P.; Peschke, P. *J. Controlled Release* **2005**, *110*, 103.
- Lencer, W. I.; Weyer, P.; Verkman, A. S.; Ausiello, D. A.; Brown, D. *Am. J. Physiol.* **1990**, *258*, 309.
- Naisbett, B.; Woodley, J. *Int. J. Pharm.* **1994**, *110*, 127.
- Reynolds, T. *J. Natl. Cancer. Inst.* **1995**, *87*, 1582.
- Wagner, E. *Adv. Drug Deliv. Rev.* **1999**, *38*, 279.
- Schwarze, S. R.; Dowdy, S. F. *Trends Pharmacol. Sci.* **2000**, *21*, 45.
- Duncan, R. *Nat. Rev. Drug Discov* **2003**, *2*, 347.
- Kopecek, J.; Kopeckova, P.; Minko, T.; Lu, Z.; Peterson, C. M. *J. Controlled Release* **2001**, *74*, 147.
- Seymour, L. W.; Duncan, R.; Strohalm, J.; Kopeček, J. *J. Biomed. Mater. Res.* **1987**, *21*, 1341.
- Cartlidge, S. A.; Duncan, R.; Lloyd, J. B.; Kopečková-Rejmanová, P.; Kopeček, J. *J. Controlled Release* **1987**, *4*, 253.
- Curti, B. D. *JAMA* **2004**, *292*, 97.
- Atkins, M. B.; Avigan, M.; Bukowski, D.; Childs, R.; Dutcher, R.; Eisen, J.; Figlin, T.; Finke, R.; Flanigan, J.; George, R.; Goldberg, D.; Gordon, S.; Iliopoulos, M.; Kaelin, O.; Lipton, W.; Motzer, A.; Novick, R.; Stadler, A.; Teh, W.; Yang, B.; King, J.; King, L. *Clin. Cancer. Res.* **2004**, *10*, 6277s.